



## COMPONENTS' AND MATERIALS' PERFORMANCE FOR ADVANCED SOLAR SUPERCRITICAL CO<sub>2</sub> POWERPLANTS (COMPASS<sub>CO<sub>2</sub></sub>)

### Particle optimization by surface treatment

**Deliverable Number 2.1**

**Version: 1**

**WP2: Development and Testing of Particles**

**Date:** November 3<sup>rd</sup>, 2022

**Deliverable type:** Report

**Dissemination level:** Public

**Lead participant:** CIEMAT



THIS PROJECT HAS RECEIVED FUNDING FROM THE EUROPEAN  
UNION'S HORIZON 2020 RESEARCH AND INNOVATION ACTION (RIA)

## AUTHORS

Name	Organization
Gema San Vicente	CIEMAT
Angel Morales	CIEMAT
Meryem Farchado	CIEMAT
Gözde Alkan	DLR
Hicham Barbri	DLR
Ceyhun Oskay	DECHEMA-Forschungsinstitut (DFI)
Michael Kerbstadt	DECHEMA-Forschungsinstitut (DFI)
Christoph Grimme	DECHEMA-Forschungsinstitut (DFI)
Mathias Galetz	DECHEMA-Forschungsinstitut (DFI)

## ABOUT THE PROJECT

COMPASsCO<sub>2</sub> is a 4-year HORIZON2020 project started on 1.11.2020. It is led by the German Aerospace Centre (DLR), with eleven additional partners from seven European countries.

COMPASsCO<sub>2</sub> aims to integrate CSP particle systems into highly efficient s-CO<sub>2</sub> Brayton power cycles for electricity production. In COMPASsCO<sub>2</sub>, the key component for such an integration, i.e. the particle/s-CO<sub>2</sub> heat exchanger, will be validated in a relevant environment. To reach this goal, the consortium will produce tailored particle and alloy combinations that meet the extreme operating conditions in terms of temperature, pressure, abrasion and hot oxidation/carburization of the heat exchanger tubes and the particles moving around/across them. The proposed innovative CSP s-CO<sub>2</sub> Brayton cycle plants will be flexible, highly efficient, economic and 100% carbon neutral large-scale electricity producers.

The research focus of COMPASsCO<sub>2</sub> is on three main technological improvements: development of new particles, development of new metal alloys and development of the heat exchanger section.

## DISCLAIMER

This project has received funding from the European Union's Horizon 2020 Research and Innovation Action (RIA) under grant agreement No. **958418**.

The content of this publication reflects only the author's view and not necessary those of the European Commission. The Commission is not responsible for any use that may be made of the information this publication contains.

# Table of Contents

LIST OF FIGURES.....	3
LIST OF TABLES .....	4
LIST OF ABBREVIATIONS .....	4
1 ABSTRACT .....	5
1 BLACK SPINEL DEPOSITION BY DIP COATING (CIEMAT) .....	7
1.1 Introduction .....	7
1.2 Experimental Procedure .....	7
1.3 Results and discussion .....	8
2 ELECTROLESS DEPOSTION OF NICKEL COATINGS (CIEMAT).....	11
2.1 Introduction .....	11
2.2 Experimental Procedure .....	13
2.3 Results and discussion .....	13
3 DEPOSITION BY RESONANT ACOUSTIC MIXER COATING (DLR) .....	15
3.1 Introduction .....	15
3.2 Experimental Procedure .....	15
3.3 Results and discussion .....	15
4 DEPOSITION BY SUSPENSION & TURBULA MIXER (DFI). .....	18
4.1 Introduction .....	18
4.2 New Coating Concept and Its Optimization.....	20
4.3 Optimized DFI Coating .....	24
5 FINAL CONCLUSIONS .....	26
6 REFERENCES.....	27

## LIST OF FIGURES

Figure 1. Saint-Gobain particles selected to CSP particle systems. ....	5
Figure 2. Granulated GEN3 particles developed by SGCREE during the project. ....	6
Figure 3. Particles located in a funnel with filter paper during coating process. ....	7
Figure 4. Effect of the spinel sintering on the $\alpha_s$ for the porous state-of-the-art particles tested. ....	8
Figure 5. Hemispherical reflectance of dense spinel coatings, on BL16/30 particles, prepared by curing method 1 and 2. ....	9
Figure 6. Effect of depositing consecutive spinel-layers on the particles tested. Method 2 of heat treatment. ....	9
Figure 7. Effect of both precursor composition and number of layers applied on GEN3 particles. Method 2 of heat treatment. ....	10
Figure 8. Variation of hemispherical reflectance as a function of the number of spinel layers (Sol A) applied. ....	11
Figure 9. Schematic representation of electroless process. ....	12
Figure 10. BL 16/30 particles before and after electroless nickel coating. ....	13
Figure 11. Hemispherical reflectance spectra of uncoated particles and two coated particles at two different Ni deposition time. ....	14
Figure 12. Schematic diagram of RAM coating process and subsequent reaction sintering. ....	15
Figure 13. Optical microscope image of BL 1630 bauxite proppants (a) before and (b) after coating with black spinel-type pigment. ....	15
Figure 14. SEM/EDX Mapping of bauxite proppant BL 1630 (a) before and (b) after black spinel coating. ....	16
Figure 15. Absorptance spectra of uncoated (BL) and black pigment coated bauxite proppants before and after thermal aging (TA). ....	16
Figure 16. SEM/EDX mapping of deep black coated granulated gen3. ....	17
Figure 17. SEM/EDX mapping of Al/deep black coated granulated gen3. ....	18
Figure 18. Macroscopic and cross-sectional SEM images of the three different particles in the as-received and as-chromized condition as well as after 120 h of isothermal exposure at 1000°C. ....	20
Figure 19. Macroscopic and cross-sectional images of the new DFI coating deposited onto granulated Gen 3 particles. ....	22
Figure 20. Cross-sectional back scattered electron (BSE) images of coated Granulated Gen 3 particles showing (a) the overview with a lower magnification, (b) the highlighted red rectangle in the previous image with a higher magnification and (c) EPMA elemental distribution maps. Please note, that the samples were sputtered with Au for the electrical conductivity. ....	23
Figure 21. Macroscopic (a) and cross-sectional (b) images and elemental distribution maps (c) of coated granulated GEN3 particles after 100 h of isothermal exposure at 1000°C. ....	24
Figure 22. Macroscopic and cross-sectional LOM images of the optimized DFI coating. ....	25

## LIST OF TABLES

Table 1. <b>S.O.A. particles (SGCREE) selection for COMPASsCO2</b> .....	6
Table 2. <b>Solar absorptance and thermal emittance calculated at 900°C of bare particles and nickel coated particles after deposition times of 4 and 12 hours</b> .....	14
Table 3. <b>Solar weighted absorptance values of coated and thermal aged granulated gen 3 particles.</b> .....	18
Table 4: <b>The components and their content in the suspension for the new coating concept of DFI.</b> .....	21
Table 5. <b>Summary of the coating technologies studied in WP2.</b> .....	26

## LIST OF ABBREVIATIONS

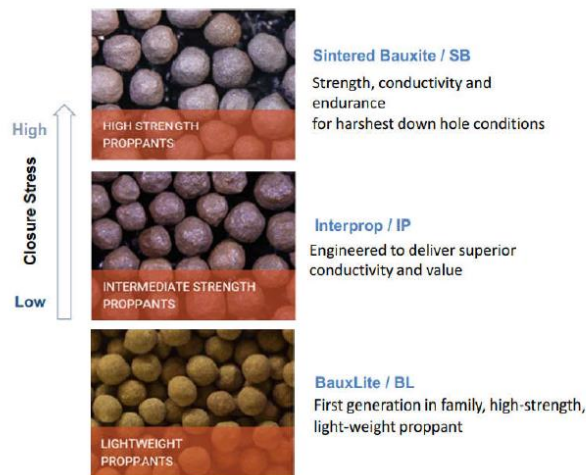
COMPASsCO2	Access Committee
CST	Concentrating Solar Thermal
EC	European Commission
EU	European Union
SGCREE	Saint Gobain
DLR	German Aerospace Centre
DFI	DECHEMA-Forschungsinstitut
CIEMAT	Centre for Energy, Environmental and Technological Research
SB	Sintered bauxite
IP	Interprop
BL	BauxLite (BL
S.O.A	State of the Art
GEN3	Generation 3
RAM	Resonant Acoustic Mixer
Wt	weight
EDX	Energy Dispersive X-ray spectroscopy
SEM	Scanning Electron Microscopy
EPMA	Electron probe microanalysis
BSE	Back scattered electron
LOM	Light optical microscope

# 1 ABSTRACT

The Work Package 2 of the COMPASsCO<sub>2</sub> project is mainly focused on three clear objectives:

- To characterise the selected particles and to assess their performance
- To tune the properties of the particles to meet the requirements of thermal stability, high absorptance and abrasion resistance.
- To understand in detail the degradation mechanisms and to model the lifetime of the particles.

Saint Gobain (SGCREE) owned in the past a business unit dedicated to the development and production of proppants but due to the market decline Saint-Gobain do not produce anymore proppants particles. These proppants particles (alumina-based) could accomplish the COMPASsCO<sub>2</sub> particles requirements and were provided from SGCREE to the partners from remaining existing stock. Three different kind of these particles (SB, IP and BL) were selected due to their properties (see Figure 1). The sintered bauxite (SB) contains the highest alumina amount among the particles selection. They also present high thermal conductivity at high temperature but a relatively low crush resistance. The interprop (IP) particles present similar properties as the SB in terms of thermal conductivity and crush resistance but the chemistry has been modified reducing the alumina content and increasing SiO<sub>2</sub>. This chemical difference modifies the optical properties. The SB product is recommended as its colour is darker. Finally, the BauxLite (BL) offers the highest crush resistance but the lowest thermal conductivity among the proposed particles.



	Chemistry (wt%)			Phase (%)			
	Al <sub>2</sub> O <sub>3</sub>	SiO <sub>2</sub>	Fe <sub>2</sub> O <sub>3</sub>	Corundum	Mullite	FeAlTiO <sub>3</sub>	Amorph
SB	>75	<10	>5	>70	<10	<6	<20
IP	>85	<18	>5	>80	<10	<5	>20
BL	55-60	<20	<9	>55	>10	<5	>20

Figure 1. *Saint-Gobain particles selected to CSP particle systems.*

Different size of these particles were available but the optimal particle size around 1 mm of diameter was established according to the heat exchanger and collector designs in the project. With this limitation, four different particles of three different compositions were chosen as state-of-the-art (S.O.A) particles to be coated by using various methods in order to improve their properties. Table 1 shows the S.O.A. particle size.

*Table 1. S.O.A. particles (SGCREE) selection for COMPASSCO2*

Particle type	Size
BL	16/30 (590 /1190 $\mu\text{m}$ )
BL	30/50 (297/590 $\mu\text{m}$ )
IP	30/50 (297/590 $\mu\text{m}$ )
SB	30/50 (297/590 $\mu\text{m}$ )

In parallel to the development of coatings on particles, SGCREE has continued developing new types of particles with improved properties (granulated and fused particles). One of them with very promising properties, the so-called granulated GEN3, has been produced in larger quantities and then they have been used to deposit coatings on them too. Granulated GEN3 particle are constituted by hematite ( $\text{Fe}_2\text{O}_3$ ) as the main phase, and have similar shape and size than S.O.A proppants particles (0.6-1.2 mm) (see Figure 2 ).

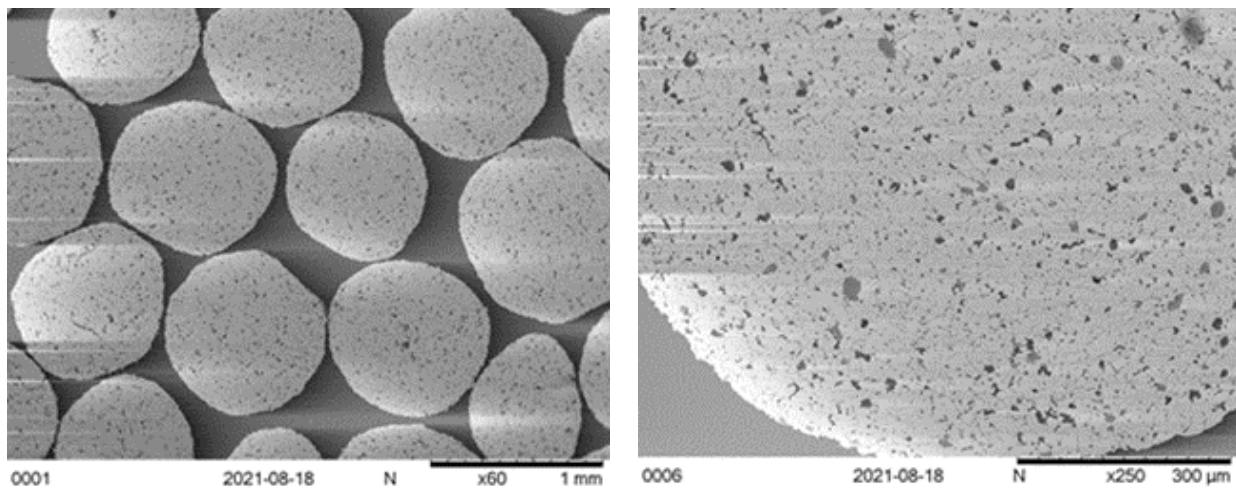


*Figure 2. Granulated GEN3 particles developed by SGCREE during the project.*

This deliverable describes the different coating deposition technologies used to improve the properties of the selected particles. CIEMAT, DLR and DFI have used different methodologies in order to deposit coatings that increases the solar absorptance, the thermal stability and abrasion resistance. The methodology and results obtained are presented in the next sections.



# 1 BLACK SPINEL DEPOSITION BY DIP COATING (CIEMAT)

## 1.1 Introduction

Among the possible materials, black-coloured transition-metal oxides with spinel-like structure could be promising candidates since they can attain high absorptance and low emittance values and display also a very high thermal stability [1],[2]. In our lab, we have developed a simple method to prepare metal oxide layers by dip-coating deposition technique [3]. A precursor solution that contains metal or metals to be deposited is prepared and then it is deposited on the substrate to be coated, mainly by substrate withdrawal at constant rate-. Finally, the coating is cured in an oven at high temperature.

## 1.2 Experimental Procedure

Metallic precursors were copper, cobalt and manganese nitrates dissolved in absolute ethanol at various concentrations. A complexing agent and a wetting additive were also added to stabilize the solution and improve the film adherence. Such solutions showed long-term stability, which made the absorber deposition both reproducible and reliable as long as the viscosity of the solution was kept constant. Two different precursor solutions have been studied in this work.

As deposition method, dip-coating process is usually employed in our laboratory to prepare solar absorbers on steel tubes and sheets, but small particles are not able to be coated in such way. Then, a new methodology has been developed, trying to imitate this coating procedure. It consists in introducing particles in a paper filter located in a glass funnel and filling the funnel with the spinel precursor solution. As solution drains through the funnel, the solution level decreases and this effect simulates the withdrawal of particles from the solution. This method presents several advantages like being simple, cost-effective, easy to scale up and versatile in operation. Figure 3 shows the deposition process on the particles.



Figure 3. *Particles located in a funnel with filter paper during coating process.*



Dip-coating deposition method is useful to prepare thin films, usually from a few nanometres up to 200 nanometres. This thickness is enough to prepare selective absorbers because interference effects enhance solar absorption but for black, non-selective absorbers it was revealed to be too thin and several layers need to be applied. In multilayer coatings, each individual coating needs to be cured at high temperature before applying next layer, so this procedure is time and energy demanding. In order to reduce energy consumption during thermal curing, two different methods were studied to cure the coatings on the particles:

Method 1: individual layers are cured 1 hour at 600°C and, after depositing last layer, complete coating is cured 1 hour at 1000°C.

Method 2: each individual layers is cured 1 hour at 1000°C.

Preliminary tests to check curing method 1 and method 2 were performed in S.O.A. particles distributed at the beginning of the project (BL16/30, SB30/50, BL30/50 and IP30/50) with a precursor solution that produces dense spinel coating [1].

### 1.3 Results and discussion

Four layers of dense spinel coating were deposited on particles using both curing methods. In Figure 4 is plotted the solar absorptance values obtained of each S.O.A. bare particles and after the 4 layers deposition by using the two curing methods. It can be appreciated that higher solar absorptance values are obtained in all S.O.A. particles using curing method 2. In the case of BL30/50 particles, similar values were obtained. Cumulative coatings prepared with curing method 1 are thinner than those prepared with method 2, as it is possible to conclude from Figure 5. In this graph, the reflectance spectra of four layers coated particles by using the two curing methods is shown. Coated particles with curing method 2 present a lower reflectance that implies both higher black coating thickness and solar absorptance.

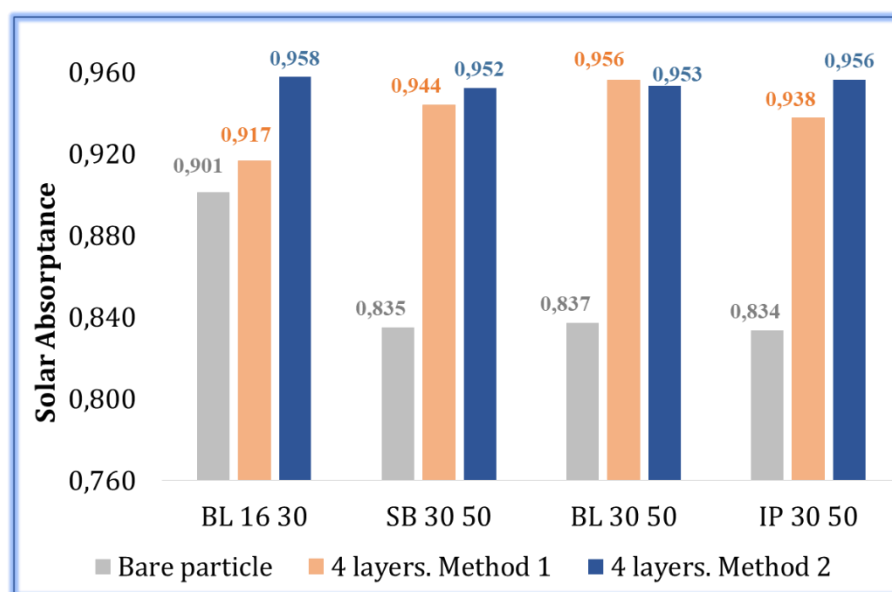


Figure 4. Effect of the spinel sintering on the as for the porous state-of-the-art particles tested.

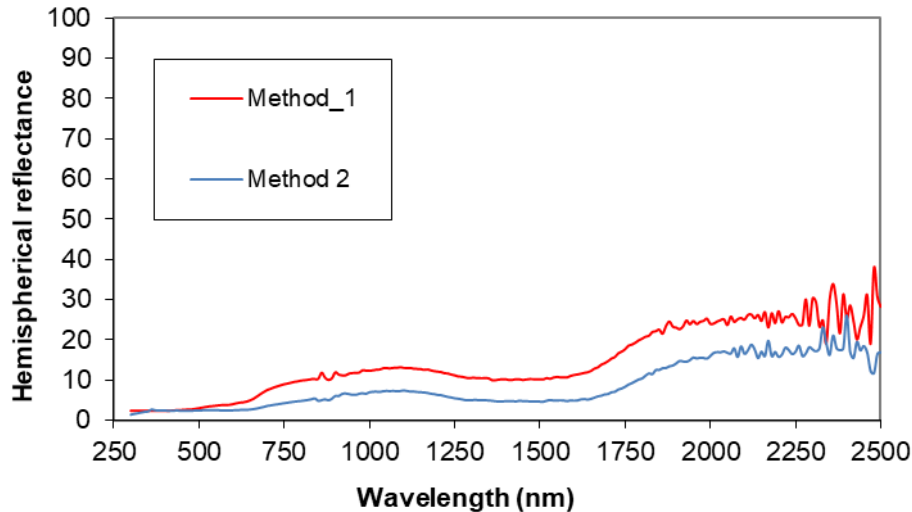


Figure 5. **Hemispherical reflectance of dense spinel coatings, on BL16/30 particles, prepared by curing method 1 and 2.**

Throughout the project, SGCREE has been developing new particles and then coatings had to be applied in the new ones. One of the most promising particles has been granulated generation 3 particles (GEN3). They present better mechanical and thermal properties. The first results showed that GEN3 particles got slightly lower solar absorptance than S.O.A. particles. In fact, solar absorptance values around 0.950 were achieved, in comparison with 0.958 obtained with BL-16/30 proppant particles.

In Figure 6, the effect of the number of layers applied in the solar absorptance values are plotted for the five different particles types [4]. Solar absorptance values increase with number of layers for all particles, except for GEN3 particles that remains stable with the fourth spinel layer.

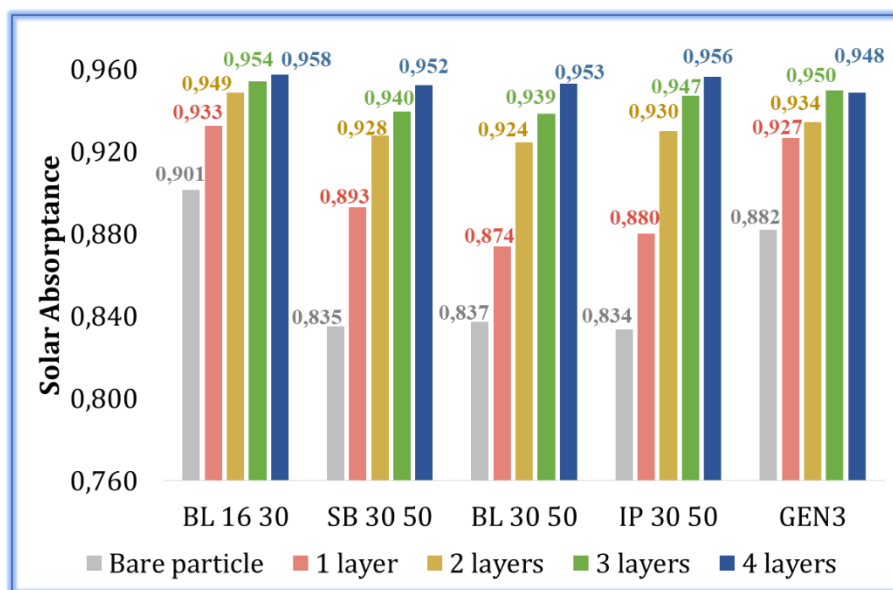
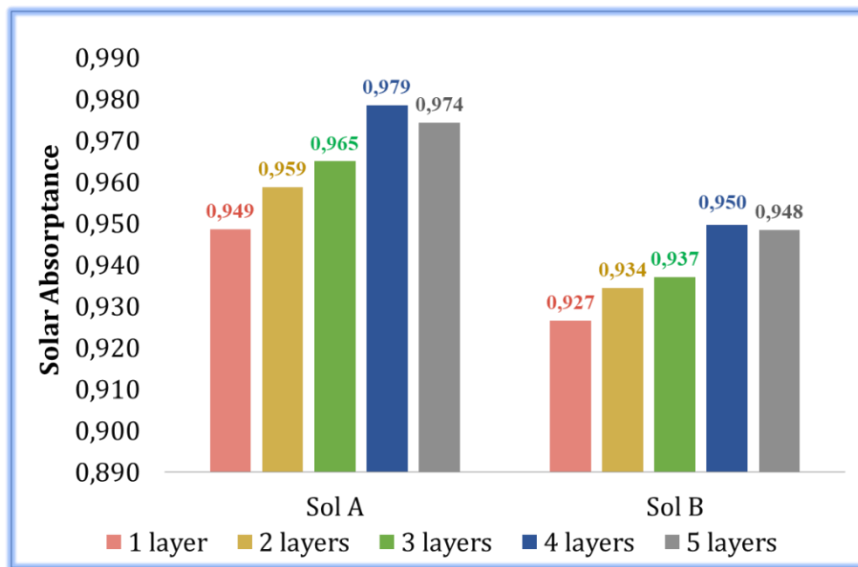


Figure 6. **Effect of depositing consecutive spinel-layers on the particles tested. Method 2 of heat treatment.**

GEN3 particles are quite dense and their surface is smooth and brilliant, so spinel coatings reproduce this surface finishing and then the solar absorptance is lower compared with the values obtained for the S.O.A particles. In order to increase solar absorptance values, a new spinel precursor solution was prepared, adding silica nanoparticles to it. The addition of these nanoparticles introduce roughness in the coating and this fact increases the solar absorptance. This precursor solution was called SOL A and the previous one that gives place to denser coatings will be then SOL B.

In Figure 7 solar absorptance values of GEN3 coated particles are shown for both precursor solutions and different numbers of consecutive layers applied. It is easily appreciated that SOL A porous spinel coating is quite absorbing and that, with only one SOL A layer, it is obtained the same solar absorptance as with four layers of SOL B dense spinel solution (0.950).



**Figure 7. Effect of both precursor composition and number of layers applied on GEN3 particles. Method 2 of heat treatment.**

Increasing the number of layers of SOL A solution implies a strong increase in solar absorptance values until fourth layer. After applying the fifth layer, the solar absorptance decreases due to a roughness reduction, as it can be deduced from spectra of Figure 8. It is observed that at higher wavelengths, five layers reflectance is lower than four layers absorber reflectance as it implies an increase in thickness. On the contrary, at lower wavelengths, the hemispherical reflectance is higher for five layers absorber than for four layers one that means that roughness has been reduced after applying the fifth spinel layer. As a conclusion, in GEN3 particles, the best optical parameters were obtained with four SOL A layers and solar absorptance values close to 0.98 have been obtained in particles produced in several batches.

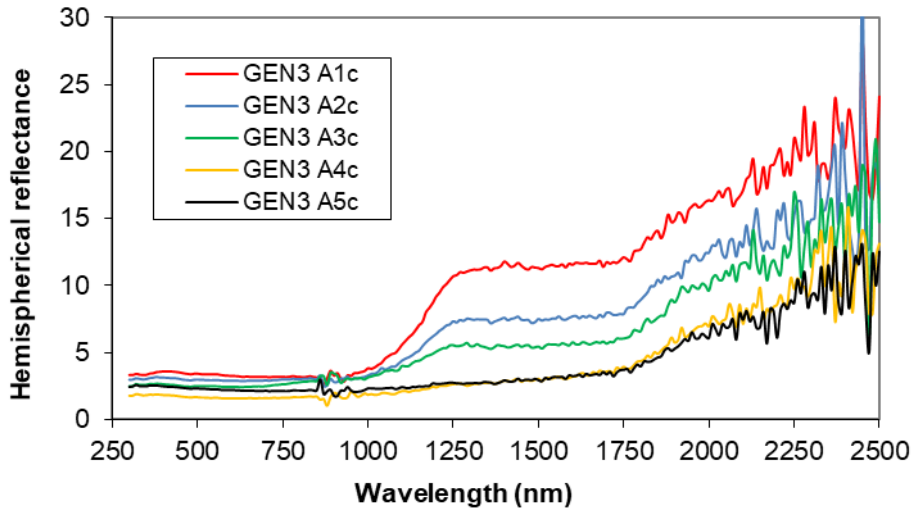


Figure 8. *Variation of hemispherical reflectance as a function of the number of spinel layers (Sol A) applied.*

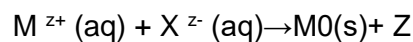
## 2 ELECTROLESS DEPOSITION OF NICKEL COATINGS (CIEMAT)

### 2.1 Introduction

Electroless plating, also known as chemical plating or autocatalytic plating, is a type of industrial chemical processes that create metal coatings on various materials by autocatalytic chemical reduction of metal cations in a liquid bath. This process is contrasted with electroplating processes, where the reduction is achieved by an externally generated electric current [5][6].

The main technical advantage of electroless plating is that it creates an even layer of metal regardless of the geometry of the surface, in contrast to electroplating, which suffers from uneven current density due to the effect of substrate shape on the electrical resistance of the bath. Moreover, electroless plating can be applied to non-conductive surfaces and parts of the object that cannot be connected to the current source.

The general reaction of electroless plating is:



where M represents the metal,  $X^{z-}$  the reducing agent, and Z its oxidized by-products (which may be liquids, solids, or gases). An schematic representation of the process is drawn in Figure 9.

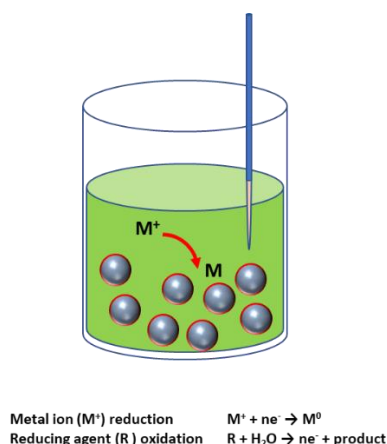


Figure 9. **Schematic representation of electroless process.**

In order to obtain a uniform solid coating of the metal on the intended surface, rather than a precipitate through the solution, the reaction requires a catalyst. This catalyst can be the substrate itself or it has to be applied on it beforehand. In fact, the reaction must be autocatalytic, so that it can continue after the substrate begins to be coated by the metal.

The use of metallic coatings on particles by electroless plating presents several characteristics that can be beneficial to this application:

- Emittance reduction due to metallic surface.
- Thermal conductivity increase with metal content and high particle porosity implies that metal can be deposited inside the particle.
- High particle porosity implies that Palladium catalyst will be strongly adhered to particle leading to metallic coatings with good adherence.

In the other hand, other characteristics can be detrimental to use electroless metal coatings on the particles:

- Solar absorptance reduction. Metals has low solar absorptance values, so another coating or mechanism needs to be used to increase solar absorptance, as it can be thermal treatment to oxidise the metal or depositing black spinel on electroless deposited metal.

Electroless deposition procedure consists of several steps:

- Preparation of metal precursor solutions. Two solutions have to be prepared: one of the solution contains nickel salts, a pH buffer and a complexing agent and the other solution contains the reducing agent. Both solutions are mixed just before particles coating procedure.
- Catalyst fixation on particles surface. A monolayer of Palladium catalyst is deposited on particles surface to start metal deposition.
- Introduction of particles in precursor electroless solution to allow metal deposition on particles.

## 2.2 Experimental Procedure

In our lab, we have experience in preparing platinum, copper, nickel and palladium electroless coatings for several applications [7], [8] and we selected nickel coatings for particles to be used in solar receptors due to its good relation price/thermal stability/deposition conditions. Platinum will have best thermal stability but its price excludes it. Palladium has good thermal stability and highest solar absorptance of these metals but its price is high too. Copper has lower thermal emissivity but its thermal stability is also low. Finally, nickel has good thermal stability, moderate price and it is the easiest material to be deposited by electroless because nickel solutions present the highest stability and it can be used during hours without nickel precipitation or poisoning.

Electroless nickel plating uses nickel salts as the metal cation source and either hypophosphite (or a borohydride like compound) as the reducer. A by-product of the reaction is elemental phosphorous (or boron) which is incorporated in the coating. For this application, hypophosphite solution has been used as reducing agent, citrate as complexing agent and sodium acetate as pH buffer.

The particles were catalysed with a palladium monolayer with a solution that contains palladium chloride, hydrochloric acid and ethanolamine.

Nickel deposition was performed at 60°C at times ranging from 1 hour to 12 hours, with particle agitation and indirect heating of the deposition container to avoid nickel deposition on it.

Stable, adherent and visually homogeneous coatings were obtained at times larger than 2 hours. In Figure 10, a picture of S.O.A. BL 16/30 proppant particles before and after nickel coating is shown.



*Figure 10. BL 16/30 particles before and after electroless nickel coating.*

## 2.3 Results and discussion

S.O.A. BL 16/30 proppant particles were selected for the study of electroless nickel deposition because they have bigger particles size and they were easier to handle and coat by this deposition method. After particle activation with Pd catalyst, they were introduced in electroless Ni bath at 60°C and after 1 hour, particles start to present a slightly metallic view. When this

electroless Ni solution is used in a dense substrate such as glass or a metal sheet, nickel metallic coating is clearly visible after 1 or 2 minutes. Higher required times to obtain an appreciable coating on proppant particles is due to particle porosity that makes that nickel deposition is produced mainly in the inner particle surface and therefore large deposition time is required.

In Figure 11, hemispherical reflectance spectra in both solar and infrared spectra is shown and it is clear the effect of nickel coating on the particles optical properties. In Table 1, solar absorptance and thermal emittance values calculated at 900°C are shown for bare particles and nickel coated particles after deposition times of 4 and 12 hours. The pursued emittance decrease is achieved with Ni coatings but solar absorptance is reduced as well. Moreover, the extremely large deposition times required to coat particles due to high porosity makes unviable to use this deposition method to improve optical properties of particles to be used in a particle receiver. In this way, with these results, the metallic electroless coatings on the particles was dismissed.

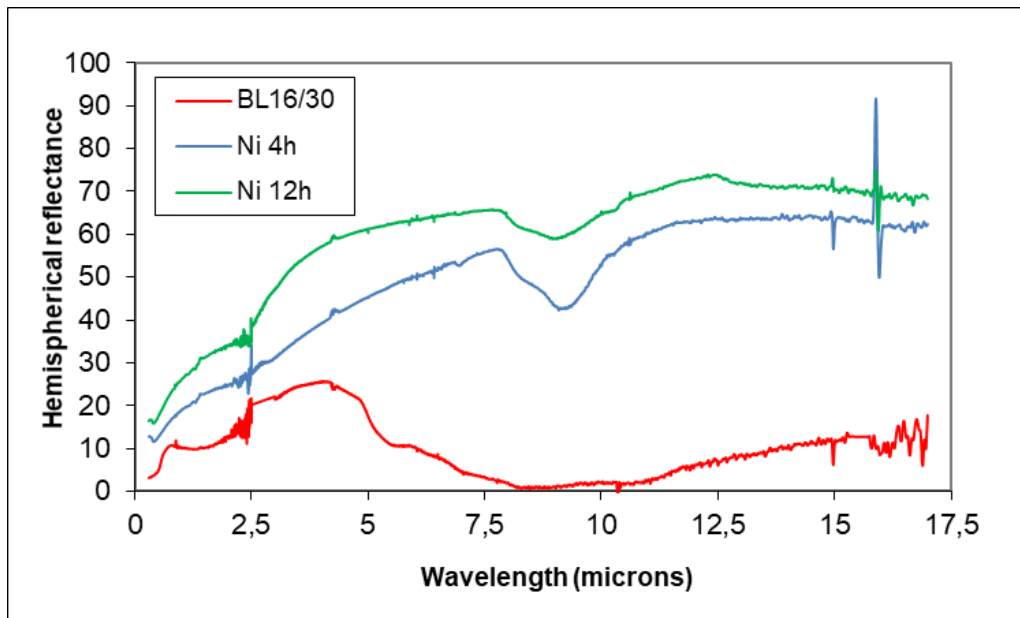


Figure 11. *Hemispherical reflectance spectra of uncoated particles and two coated particles at two different Ni deposition time.*

Table 2. *Solar absorptance and thermal emittance calculated at 900°C of bare particles and nickel coated particles after deposition times of 4 and 12 hours*

	Deposition time		
	0h	4h	12h
$\alpha_s$	0,913	0,833	0,770
$\epsilon_{900C}$	0,838	0,630	0,497



## 3 DEPOSITION BY RESONANT ACOUSTIC MIXER COATING (DLR)

### 3.1 Introduction

In this section, DLR uses a novel dry coating process, utilizing a resonance acoustic mixer, to deposit a commercial deep-black pigment powder on the S.O.A. proppants particle surface followed by heat treatment and reaction-bonding.

### 3.2 Experimental Procedure

In a typical coating experiment, 1 wt. % of black pigment and 99 wt. % proppants were poured in a plastic vessel and viciously agitated by the RAM running at 100 g acceleration. Owing to the electrostatic attraction between pigment powder and proppant particles, a uniform pigment layer on top of the S.O.A surface is achieved after 10 seconds of agitation only. Subsequently a heat treatment at 1200 °C for 2 hours was applied to ensure the bonding of pigments to the proppant surface. A schematic diagram of the process is represented in Figure 12.

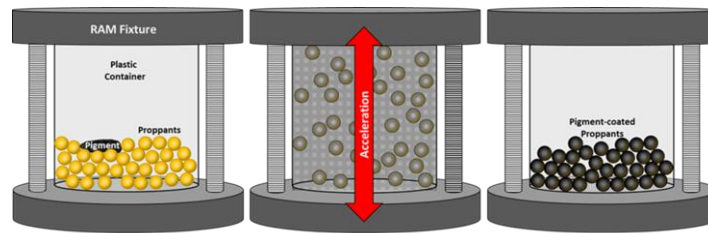


Figure 12. *Schematic diagram of RAM coating process and subsequent reaction sintering*

### 3.3 Results and discussion

Figure 13 depicts the S.O.A. proppants surface before and after coating in a comparative manner. Whereas the uncoated proppants show a yellow-to-brown, widely scattering colour (Figure 13a), the homogenous blackening of the pigment coated proppants is evident (Figure 13b).

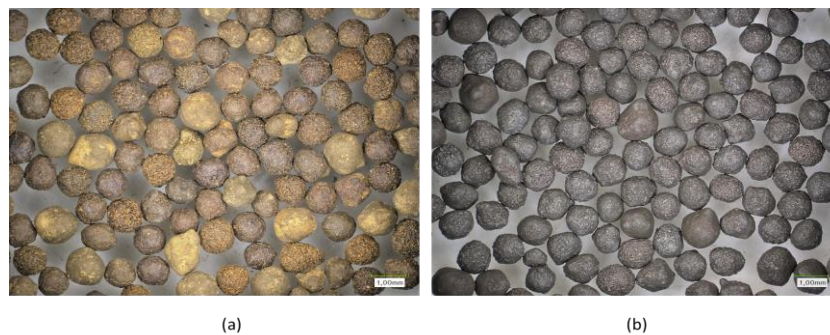
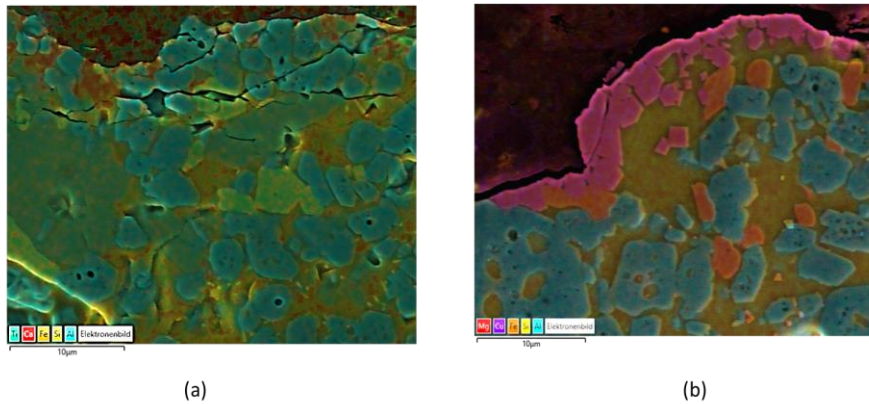


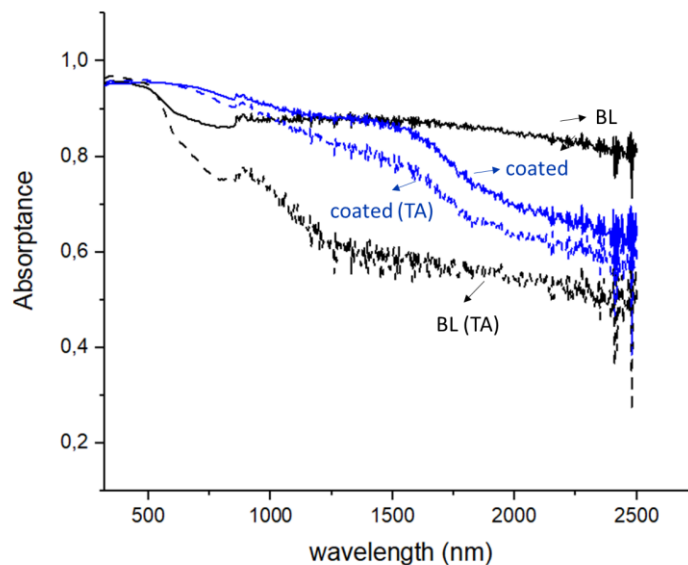
Figure 13. *Optical microscope image of BL 1630 bauxite proppants (a) before and (b) after coating with black spinel-type pigment*

Figure 14 represents microstructural features and overlaid EDX mappings of BL proppant before and after deep-black pigment coating. Typical proppant morphology comprising corundum particles, iron bearing crystals and surrounding glass matrix was not affected substantially from the coating process:



**Figure 14. SEM/EDX Mapping of bauxite proppant BL 1630 (a) before and (b) after black spinel coating**

A key for the performance of black-pigment coated proppants in CSP applications is their optical behaviour. The absorbance spectra in the range of 320–2500 nm of BL proppants in as received condition, after coating and thermal aging are plotted in Figure 15.



**Figure 15. Absorbance spectra of uncoated (BL) and black pigment coated bauxite proppants before and after thermal aging (TA).**

The solar weighted absorbance has been calculated according to ASTM 173d standards. The solar absorbance value of 0.89 for BL in as-received condition has significantly decreased to 0.78 after 1-week thermal aging. The black spinel coating enhanced slightly the solar absorbance in the as received state from 0.89 to 0.92. Beyond this increase, optical analysis reveals the stability of coated proppants' absorbance after thermal aging with the value of

0.91. In consistent with microstructural findings, the spinel #2 layer at the surface remains stable through thermal aging, which is considered very promising for efficient and long-term stable CSP operation of proppants.

The same deep black pigment with same experimental conditions were applied to the granulated GEN3, which includes hematite ( $\text{Fe}_2\text{O}_3$ ) as the main phase. Even after two layers of coating, the colour of the GEN3 particles has not changed significantly. SEM/EDX analysis were performed as given in Figure 16.



Figure 16. **SEM/EDX mapping of deep black coated granulated gen3**

EDX mapping of the cross section revealed a significant diffusion of Fe and Cu components into the hematite structure, which results in colour loss.

During the coating of the S.O.A. proppants, it was found out that, Fe-Cu-Mn spinel pigment reacts with Al component of bauxite and forms a more stable Al including spinel. In order to utilize this favourable reaction between deep black and aluminium, for a more efficient coating of granulated gen 3 particles, metallic Al was mixed with deep black and applied to the particle surface by RAM. Metallic Al with the melting point of 650 °C has also favoured the homogenous distribution of deep black through the particle surface. SEM/EDX analysis of the coated granulated GEN3 particles with Al incorporation is given below (Figure 17) and it shows that the diffusion of pigment to the inner parts of the particle was prevented.

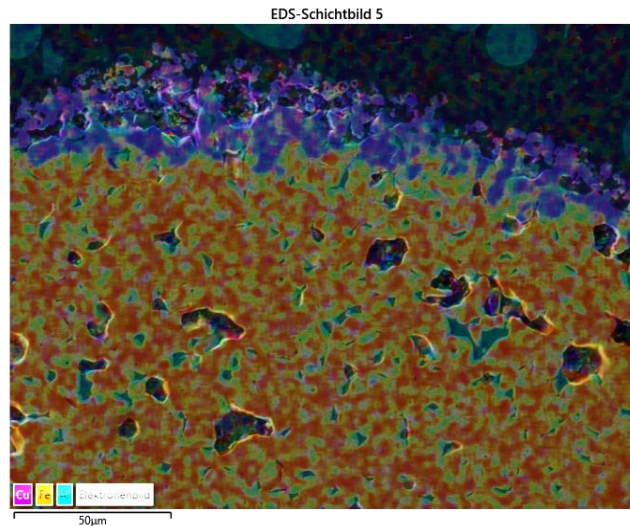


Figure 17. **SEM/EDX mapping of Al/deep black coated granulated gen3**

In Table 3, the solar weighted absorptance values obtained before and after coating the granulated GEN3 particles are recorded. It was revealed that even after 1 week thermal aging at 1000 °C, the particles had conserved their solar absorptance values.

Table 3. **Solar weighted absorptance values of coated and thermal aged granulated gen 3 particles.**

	Bare granulated GEN3 particles	Coated granulated GEN3 particles
initial	0.88	0.93
1000 °C, 1 week	0.88	0.93

## 4 DEPOSITION BY SUSPENSION & TURBULA MIXER (DFI).

### 4.1 Introduction

The preliminary approach of DFI aimed at the deposition of Cr-rich coatings onto the particles by the industrially well-established method of pack cementation. The methodology has been described in detail in the 1<sup>st</sup> periodic report of the project. The described methodology has been utilized to manufacture Cr-rich coatings on three different S.O.A particles type, namely the BL 16/30, BL30/50 and SB 30/50. Chromium enrichment at the surface of the particles was thought to lead to the in-situ formation of Cr-rich spinel oxides at service temperatures and since the coating provides a Cr-reservoir, these oxides were thought to be healed in case of formation of cracks and/or spalled areas. Figure 18 depicts the macroscopic and cross-sectional images of the three selected particles in the as-received and as-coated conditions as well as the coated particles after 120 h of isothermal exposure at 1000°C. Independent from the particle type, all particles appeared in a dark-grey colour after the coating deposition, they

changed to a greenish colour after the isothermal exposure. The cross-sectional images showed the local enrichment of metallic Cr at the surface of the particles (confirmed by EDX, not shown here), particularly much more pronounced for BL 16/30, whereas other particles showed lesser enrichment of metallic Cr. Especially on BL 16/30, there are some gaps visible, which indicate the spallation of the coating. This can be associated with the thermally induced stresses during the cooling from the coating manufacturing temperature due to the mismatch of thermal expansion coefficients of the coating and the substrate. After the isothermal exposure at 1000°C for 120 h, the coated particles, again independent of the particle type, all showed a dark green colour, which is typical for Cr<sub>2</sub>O<sub>3</sub>. The formation of chromia can be attributed to the presence of metallic Cr within the as-deposited coatings. Instead of the formation of a metallurgical bond to the substrate, as it is the case for diffusion coatings deposited on metallic alloys, metallic Cr was loosely deposited from the gaseous phase to some extent onto the surface of the particles, which oxidized during exposure and formed Cr<sub>2</sub>O<sub>3</sub>. DFI carried out optimization trials with the pack cementation coatings on the S.O.A proppants to increase the coating adhesion to the substrate, however the results were unfortunately unsatisfactory. Hence, a new coating concept was proposed to the project partners within the WP2 monthly meeting on 13<sup>th</sup> of May 2022. This new concept is elucidated in detail in the following sections.



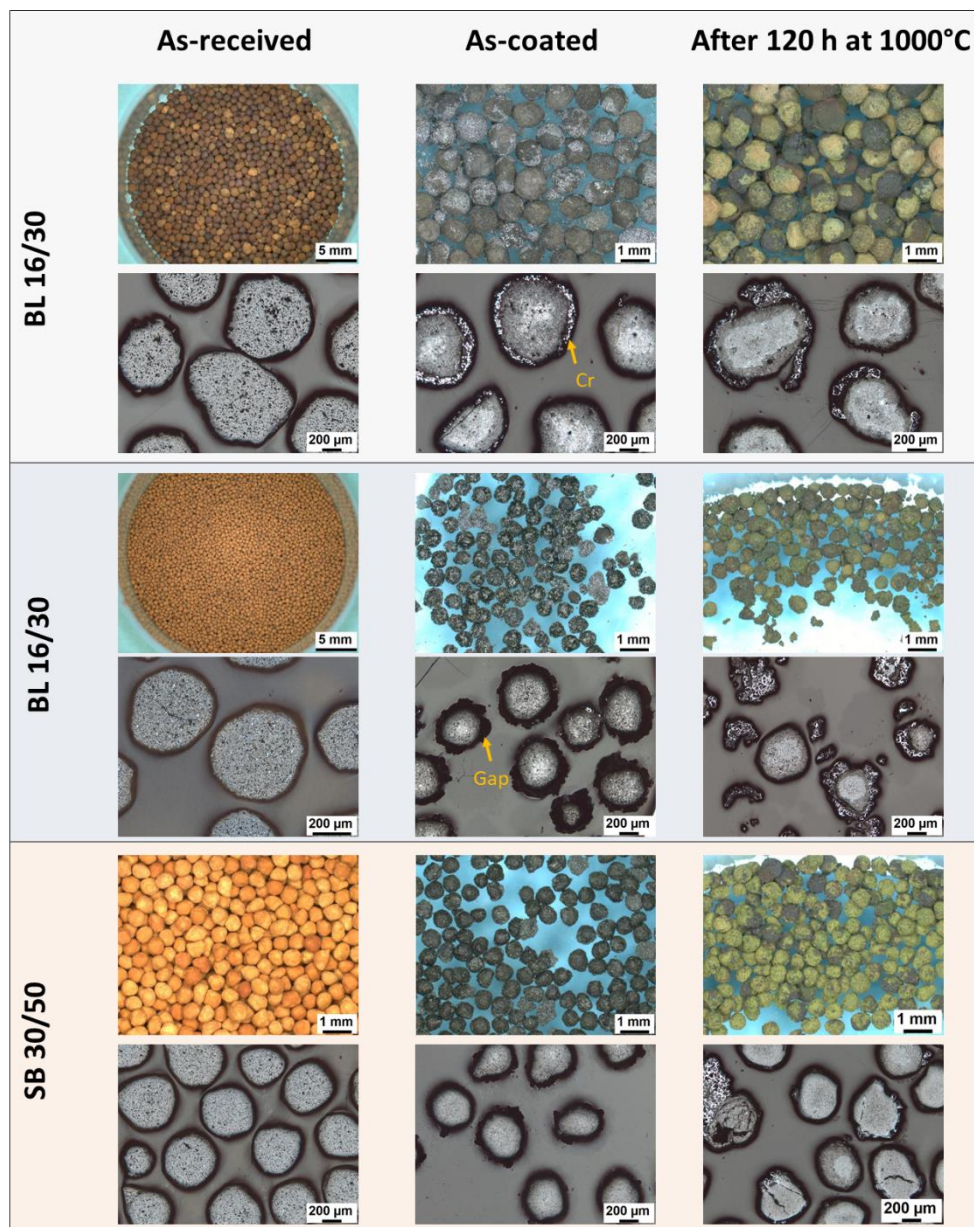


Figure 18: *Macroscopic and cross-sectional SEM images of the three different particles in the as-received and as-chromized condition as well as after 120 h of isothermal exposure at 1000°C.*

## 4.2 New Coating Concept and Its Optimization

The new coating concept of DFI involves a similar coating deposition process as CIEMAT and DLR coatings and utilizes a coating deposition from a liquid phase, namely a suspension, in which industrial black pigments are dispersed in a reactive methyl phenyl silicone resin. The components and their content in the suspensions is given in

Table 4.

*Table 4: The components and their content in the suspension for the new coating concept of DFI.*

Component	Content [wt.%]
AC900 (Resin)	47,7
TEGO Dispers (Dispersion agent)	2,4
Bentone SD-1	1,8
Mica	18,8
AEROSIL R972	1,8
Ethanol	27,5
HEUCODUR 953 (black pigments)	25
TEGO Cure 100 (curing agent → curing at RT)	5

The suspension contains the Silikophen® AC 900 resin, the dispersion agent, TEGO® Dispers, other coating additives such as Bentone SD-1, Mica and Aerosil® R 972 and ethanol as the solvent. After the preparation of this suspension, the industrial black pigments ( $\text{CuCr}_2\text{O}_4$ ) with the trademark name, Heucodur®953 were added to the suspension with a content of 25 wt.% based on the pristine suspension. Subsequently, the suspension was mixed using a Turbula® mixer for 30 minutes for the homogenization of the mixture. Thereafter the novel curing agent, TEGO® Cure 100 was added to the suspension with a content of 5 wt % again based on the pristine mixture. After the addition of the curing agent particles were added to the suspension and the suspension containing the particles (with a weight suspension/particle weight ratio of 5:1) was mixed again using the Turbula® mixer for 2 hours. The original idea aimed at the deposition of the coating onto the particles during the mixing process. Since the novel curing agent enables the curing of the coating or in other words the formation of silica chains from the reactive silicone resin at room temperature, the coating deposition can be finalized during the mixing process.

Due to the time constraints, the new coating deposition method by DFI involving the preparation of the aforementioned suspension and the deposition and coating formation process with one step by the rotary mixing was not applied on the proppants, but onto the novel granulated GEN3 particles. Figure 19 shows the macroscopic and cross-sectional images by light-optical microscopy of the coated granulated GEN3 particles. Significant improvement of the absorptivity via the dark colour noted, the particles agglomerated strongly. The cross-sectional images under polarized light highlight, the bridging of the particles together by suspension remnants. Evidently, the curing process or the formation of the silica chains took place during mixing, which was the target of this coating manufacturing process, however, the suspension rests between the particles led to their agglomeration.



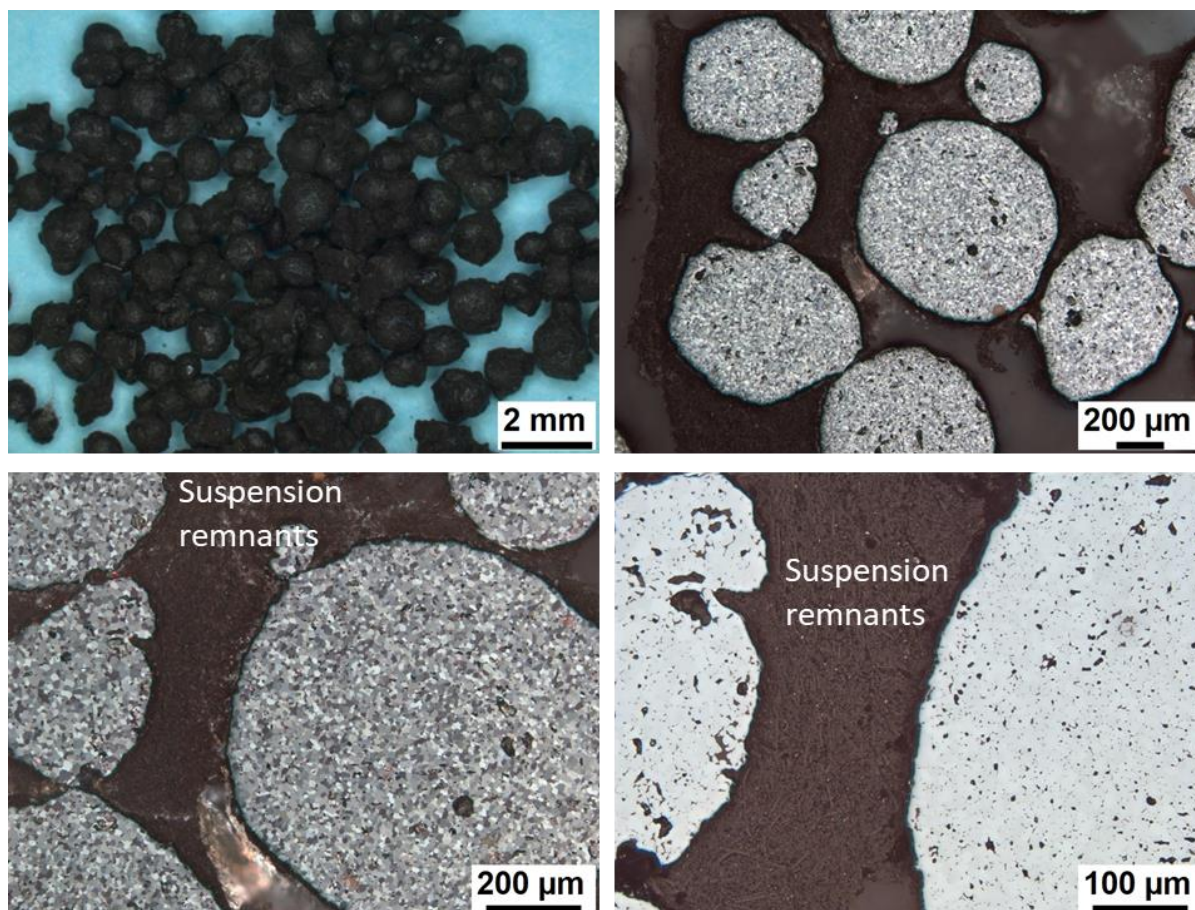


*Figure 19: Macroscopic and cross-sectional images of the new DFI coating deposited onto granulated Gen 3 particles.*

With the agglomeration being noted, the very dark colour of the particles was considered to be promising for their absorptance. Therefore, the chemical composition and the microstructure of the coatings were decided to be analysed in detail using electron probe microanalysis (EPMA). Figure 20 illustrates the cross-sectional back scattered electron (BSE) images of coated granulated Gen 3 particles and the elemental distribution maps obtained by EPMA. The overview image shows a non-homogeneous coating thickness on the selected representative area for imaging. It should however be noted that, the cross-sectioning of round particles might have led to the appearance of different coating thicknesses. The higher magnification image (see Figure 20.b) shows the enrichment of Cu and Cr inside a silica matrix. The presence of Cu and Cr inside coating originated from the  $\text{CuCr}_2\text{O}_4$  spinel, which was used as the black pigments. The formation of the silica matrix verified the completion of the curing process of the coating.

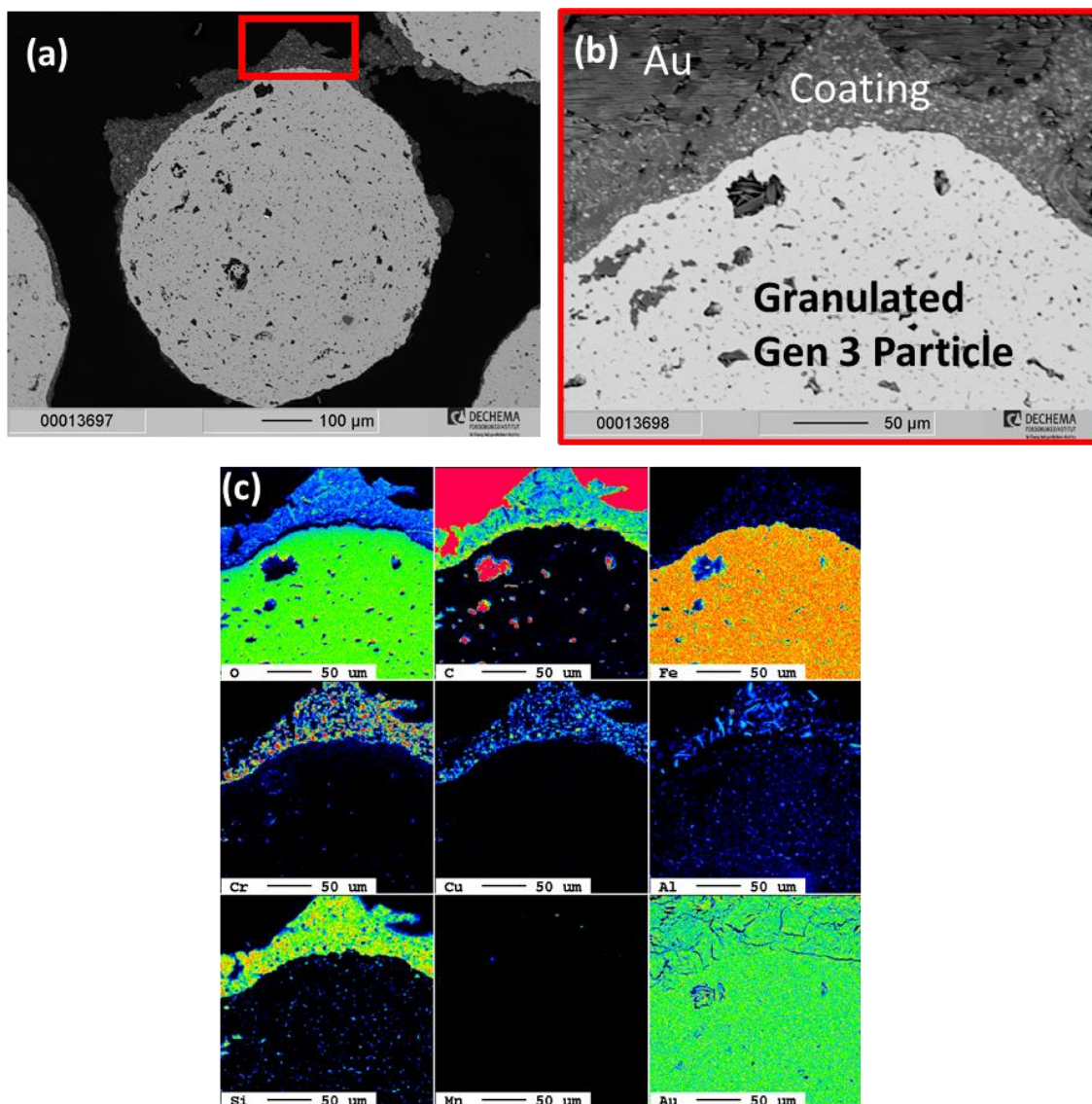


**Figure 20: Cross-sectional back scattered electron (BSE) images of coated Granulated Gen 3 particles showing (a) the overview with a lower magnification, (b) the highlighted red rectangle in the previous image with a higher magnification and (c) EPMA elemental distribution maps. Please note, that the samples were sputtered with Au for the electrical conductivity.**

Furthermore, the coated particles did not show significant degradation after 100 h of isothermal exposure at 1000°C (see Figure 21). Both the colour and the chemical composition of the particles did not change significantly.  $\text{CuCr}_2\text{O}_4$  spinel was still present inside the silica matrix at the surface of the coatings. Disregarding the strong agglomeration of the particles during the coating process, their chemical composition, dark colour and the fact that, they did not degrade significantly during isothermal exposure, were considered to be very promising aspects. Owing to the fact that, such a strong agglomeration of the particles will lead to a significant reduction in their functionality, an optimization of the coating process has been undertaken at DFI without changing the suspension composition.



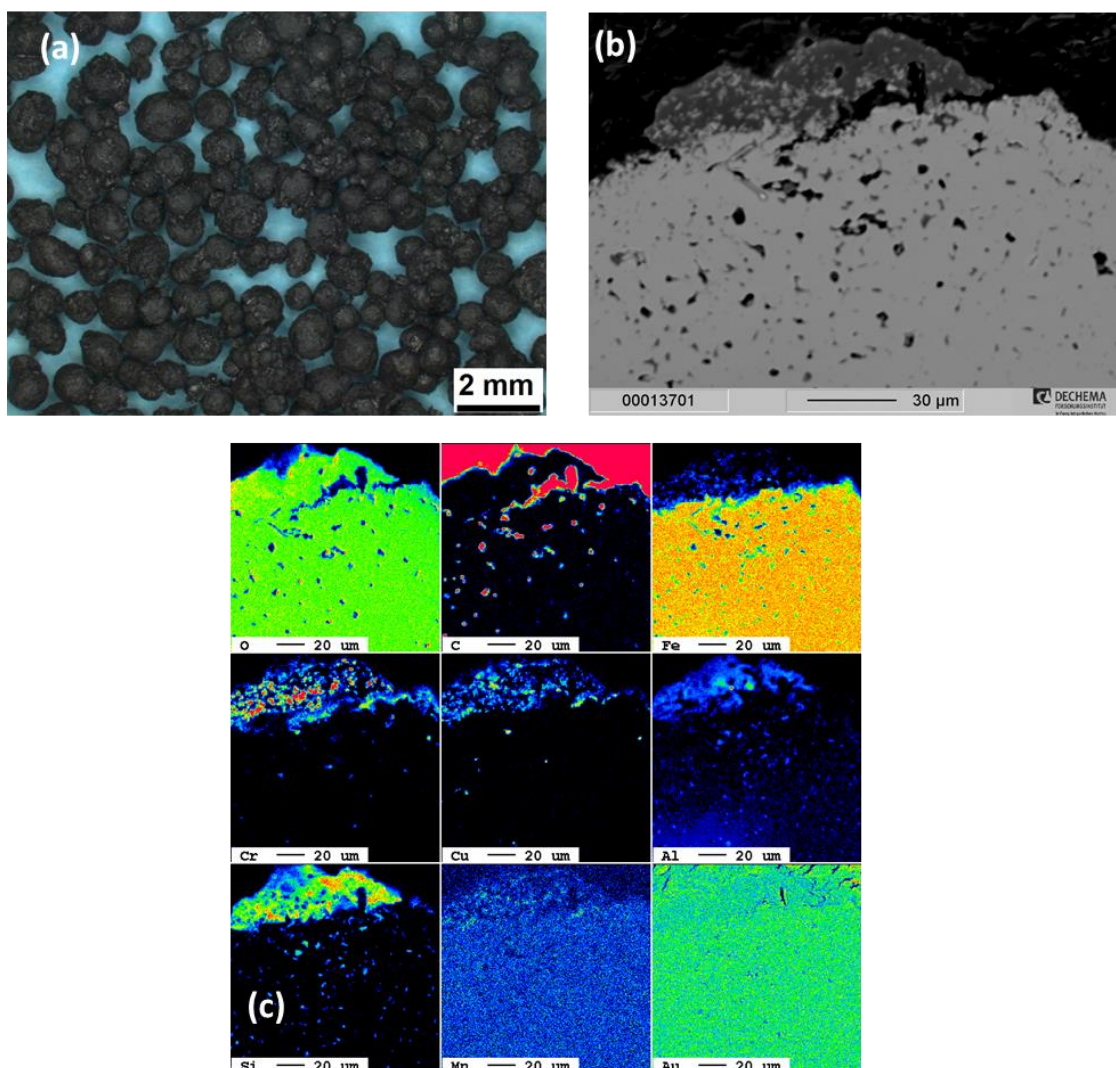


**Figure 21: Macroscopic (a) and cross-sectional (b) images and elemental distribution maps (c) of coated granulated GEN3 particles after 100 h of isothermal exposure at 1000°C.**

The agglomeration of the particles probably originated from the rotary mixing process, which provided apparently sufficient time for the particles being bridged by the suspension remnants. Instead of a mixing process, in which the particles should be immersed in the suspension, DFI decided to utilize the air-spraying method, in which the amount of suspension deposited onto the particles can be controlled. While the particles were kept in constant movement on an automated sieve with a low vibration frequency to avoid the abrasion of particles, the suspension (see Table 4 for the chemical composition) was air-sprayed onto the particles. Three layers were sprayed onto the particles, with each layer step including a short period of drying of the particles, with the suspension rests being sieved. A detailed microstructural characterization was undertaken, which involved the mounting of the coated particles in plexy-glass and the conventional metallographic preparation of the cross-sections as well as light-optical microscopic imaging. This microstructural characterization of the optimized DFI coating is shown in the following section.

### 4.3 Optimized DFI Coating

Figure 22 shows the macroscopic images and cross-sectional light optical microscope (LOM) images of the optimized DFI coating. Evidently, the dark colour of the coating, which was deposited by the rotary mixing method (compare with Figure 20) could be maintained also by the air-spraying method of the optimized coating. Furthermore, the cross-sectional images highlight a significant improvement in the homogeneity of the coating thickness and hindering the agglomeration of the particles. With the amount of suspension deposited onto the particles reduced and better controlled via the air-spraying, the agglomeration could be hindered to a great extent. The utilization of an automated sieve during the slurry deposition of the coating might have also played a keen role in the elimination of the strong agglomeration of the particles, which was observed by the rotary mixing method. Probably, the suspension remnants, which were bridging the particles and forming the silica chains during the mixing, was hindered by the utilization of the sieve. The microstructural characterization of the optimized coating was presented to the partners during the WP2 monthly meeting on 15.09.2022.

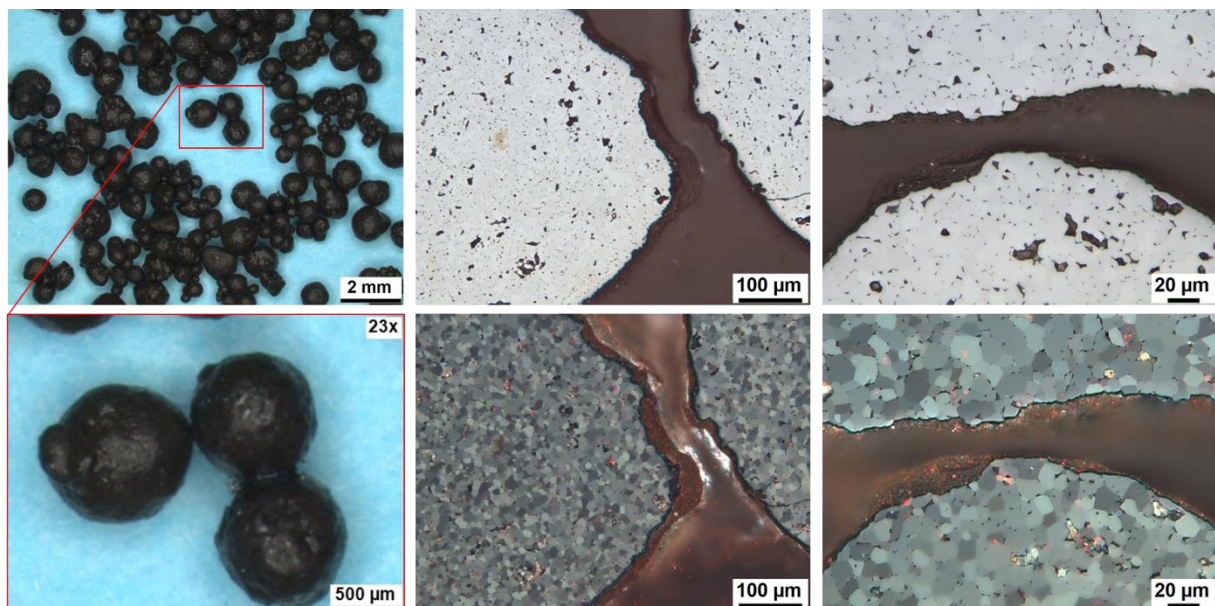


*Figure 22: Macroscopic and cross-sectional LOM images of the optimized DFI coating*

DFI deposited the optimized coating on 1200 g of granulated GEN3 particles and sent to partners on 17.08.2022 for the testing of particles to characterize their service relevant properties such as absorptance and abrasion resistance. Likewise, DFI has received the coated particles by CIEMAT (see section 1) and DLR (see Section 3) for further characterization and testing. DFI will conduct high temperature in-situ XRD analysis to characterize the coating phases during heating and cooling as well as thermocyclic exposure of particles with one cycle consisting of a dwell time of 1 h at 1000°C and cooling to room temperature. Such exposure tests are planned to simulate the build-up of thermally induced stresses in the coatings and their effect on the adhesion of the coatings.

## 5 FINAL CONCLUSIONS

The experimental details and results about coating deposition from CIEMAT, DLR and DFI are been compiled in this document. The possibility of depositing coatings on the particles to modify their properties have been successfully proven. It should be noted that the coatings compositions and methodologies are dependent of the particles used and then it was necessary to adjust both depending of the particles type. Table 5 shows the summary of all the methodologies tested.

Table 5. *Summary of the coating technologies studied in WP2.*

Partner	Coating Composition	Method	Max. Solar absorptance in GEN3	Achievement
CIEMAT	CuMnCoO <sub>x</sub> and CuMnCoO <sub>x</sub> /SiO <sub>2</sub>	Dip Coating	0.98	<b>successful</b>
CIEMAT	Ni	Electroless	-	unsuccessful
DLR	FeCuMnO <sub>x</sub> and FeCuMnO <sub>x</sub> /Al	Resonant acoustic mixer coating	0.94	<b>successful</b>
DFI	Cr-rich	Cementation	-	unsuccessful
DFI	CuCr <sub>2</sub> O <sub>4</sub>	Suspension & turbula mixer	-	<b>successful</b>
DFI	CuCr <sub>2</sub> O <sub>4</sub>	Suspension & air spraying	0.97	<b>successful</b>

**CIEMAT** has applied electroless method to deposit nickel coating on the particles to decrease their thermal emittance as it was proposed in the project proposal. The porous nature of the particles made very difficult to apply the coating in the surface as it was introduced in the inner of the particles. Consequently, very long reactions times were necessary to achieve the surface coating of the particles. On the other hand, the decrease in particle thermal emittance brought with it an increase in solar absorptance. With these results this coating and this method was stopped. Then the application of CuMnCo spinel by dip coating was studied. The coating composition and deposition conditions was optimized to obtain the higher solar absorptance values (0.98 vs 0.88 (uncoated GEN- particles)).

**DLR** has applied a novel dry coating process, utilizing a resonance acoustic mixer to deposit FeCuMn spinel on the S.O.A. and GEN3 particles. Microscopy studies have shown the successful deposition on the particles. It has been also seen that the Al content in S.O.A particles improved the stability of the coating. In this way, the coating composition was modified to incorporate Al when particles without Al in its composition are coated. The increase in GEN3 particles solar absorptance has been also achieved with enhanced thermal resistance.

The application of Cr rich coatings by pack cementation was proposed and studied by **DFI** with the aim of modifying the particles characteristics. After some tests, issues with the green chromia formation and the adherence of the coating in the particles led to the abandonment of this strategy. However, DFI approached a new coating concept based on CuCr<sub>2</sub>O<sub>4</sub> pigments by suspension & turbula mixer method. The suspension was optimized to obtain

black and adherent coatings on the GEN3 particles. Agglomeration of coated particles during isothermal exposure at 1000°C was solved by using air-spraying application method. Solar absorptance values of 0.97 were obtained with the optimized coating on GEN3 particles.

As a general conclusion, various coatings applied by different methodologies has been successfully achieved. The optimized particles produced by the partners have been distributed to the partners for complete characterisation and evaluation.

## 6 REFERENCES

- 
- [1] Avila A., Morales A., Monterreal R., Fernández--Reche J.; “Non-selective coating for porous materials used for solar thermal applications”; SOLARPACES 2018: July 2019 AIP Conference Proceedings 2126(1):030007.
- [2] “Raising the Lifetime of Functional Materials for Concentrated Solar Power Technology (RAISELIFE)”; H2020 European Union NMP-16-2015, Grant agreement: 686008.
- [3] Morales A., Process to deposit metal and metal oxide coatings, European Patent: EP1321539 (A3).
- [4] Farchado M., Tordesillas R., San Vicente G., Germán N. and Morales A. “Optimization of Spinel Absorber Coatings for CSP Particle Receivers”. Presented in SOLARPACES 2022. September 27-30,2022, Albuquerque, NM, USA.
- [5]. Mallory G. O and Hajdu J. B., editors (1990): Electroless plating: fundamentals and applications. 539 pages. ISBN 9780936569079
- [6] Shipley Jr Charles R. (1984): "Historical highlights of electroless plating". Plating and Surface Finishing, volume 71, issue 6, pages 24-27. ISSN 0360-3164
- [7] Ruiz E., Cillero D., Martínez P.J., Morales A., San Vicente G., de Diego G., Sánchez J.M. “Electrochemical synthesis of fuels by CO<sub>2</sub> hydrogenation on Cu in a potassium ion conducting membrane reactor at bench scale”; Catalysis Today 236, 108-120; 2014
- [8] Ruiz E., Cillero D., Martínez P.J., Morales A., San Vicente G., de Diego G., Sánchez J.M.; Bench-scale study of electrochemically assisted catalytic CO<sub>2</sub> hydrogenation to hydrocarbon fuels on Pt, Ni and Pd films deposited on YSZ” Journal of CO<sub>2</sub> Utilization 8, 1-20; 2014